Journal of Diabetes and Its Complications 33 (2019) 278–288

Contents lists available at ScienceDirect

Journal of Diabetes and Its Complications

journal homepage: WWW.JDCJOURNAL.COM

Lower cardiovagal tone and baroreflex sensitivity associated with hepatic insulin resistance and promote cardiovascular disorders in Tibetan minipigs induced by a high fat and high cholesterol diet

Yongming Pan, Yili Rong, Junjie Huang, Keyan Zhu, Jiaojiao Chen, Chen Yu, Minli Chen *

Comparative Medical Research Institute, Experimental Animal Research Center, Zhejiang Chinese Medical University, Hangzhou 310053, China

ARTICLE INFO

Article history:
Received 18 September 2018
Received in revised form 4 December 2018
Accepted 27 December 2018
Available online 4 January 2019

Keywords:
Hepatic insulin resistance
Baroreflex sensitivity
Cardiovagal tone
Hepatic steatosis
High-fat/cholesterol diet
Tibetan minipig

ABSTRACT

Aims: A long-term high-fat/cholesterol (HFC) diet leads to hepatic insulin resistance (IR), which is associated with autonomic dysfunction and cardiovascular diseases risk increasing. However, whether this occurs in Tibetan minipigs remains unknown. We tested that a long-term HFC diet caused hepatic IR and promote cardiovascular disorders in Tibetan minipigs, and are associated with the reduction of cardiovagal tone and baroreflex sensitivity (BRS).

Methods: Male Tibetan minipigs were fed either a standard diet or a HFC diet, and were euthanized at 12 weeks. Thereafter, the minipigs were tested for biochemical blood indices, glucose tolerance, blood pressure, heart rate variability (HRV), BRS, and insulin receptor substrate (IRS)-associated gene and protein expression levels, as well as cardiac function.

Results: HFC-fed minipigs developed IR by increasing body weight, total cholesterol, fasting blood glucose and insulin levels, and nonesterified fatty acid (NEFA) and high sensitive C-reactive protein (hs-CRP) levels, glucose intolerance. Increased adipose cell size, hepatic fat deposition, malondialdehyde (MDA) content and NEFA level, down-regulation of IRS1, IRS2, PI3K, Akt, p-Akt, Glut2 and PGC1α expression concomitant with up-regulation of mTOR, GSK3β, TNF-α, FOXO1, p-mTOR and p-p70S6K expression in the liver tissue, as well as hypertension and left ventricular diastolic dysfunction were observed in HFC-fed minipigs. HRV parameters and BRS values were further significantly reduced. Furthermore, multiple linear regression analysis showed that the development of hepatic IR toward cardiovascular disease was associated with low HFnu, RMSSD, BRS and LV −dp/dtmax, high NEFA, high hepatic TG content.

Conclusion: These data suggest that HFC-fed Tibetan minipigs develop hepatic IR and promote cardiovascular disorders, and are associated with lower cardiovagal tone and BRS.

1. Introduction

Modern medicine is meeting the challenges of increasing cardiovascular diseases due to hyperlipidemia, hypertension, diabetes and metabolic syndrome,[1,2] which has seriously affected people's quality of life and life expectancy and brought a heavy social and clinical burden. However, its underlying etiology and pathogenesis have not yet been fully elucidated. Insulin resistance (IR), a pathological state that refers to a decrease in the effect of insulin on peripheral tissues,[3] has to do with unhealthy lifestyles such as overeating, obesity and lack of physical activity. Recently, IR has been considered to be the core of various metabolic abnormalities and has been proved closely related to the development of type 2 diabetes and cardiovascular disease.[4]

Liver is the most important organ involved in the regulation of glycolipid metabolism and a sensitive target organ of insulin, and many functions of the liver are strictly controlled by circulating hormones such as insulin. Hepatic IR results in fasting and postprandial hyperglycemia, which in turn exacerbates insulin sensitivity and aggravates IR in peripheral tissues.[5] Recently, it has been found that hepatic IR can directly or indirectly promote the development of cardiovascular disease,[6] which increases the risk of diabetes and cardiovascular diseases through conventional mechanisms (such as impaired insulin signaling, dyslipidemia, hyperglycemia) and the release of inflammatory mediators.[7–9] In addition, autonomic dysfunction is related to IR and cardiovascular disease.[10] Sympathovagal imbalance (SVI) and depressed heart rate variability (HRV) are associated with cardiovascular morbidity and mortality,[11] while changes in SVI are associated with metabolic abnormalities.[12] Baroreflex sensitivity (BRS) is the most important

* Corresponding author at: Comparative Medical Research Institute, Experimental Animal Research Center, Zhejiang Chinese Medical University, No. 548 Binwen Road, Binjiang District, Hangzhou 310053, China.
E-mail addresses: pym@zcmu.edu.cn (Y. Pan), ryl@zju.edu.cn (Y. Rong), cmli991@zcmu.edu.cn (M. Chen).

https://doi.org/10.1016/j.jdiacomp.2018.12.014
1056-8727/

neuromodulation mechanism of cardiovascular homeostasis.[13,14] Lower BRS was seen in obesity, diabetes, hypertension, coronary atherosclerosis, nonalcoholic fatty liver disease (NAFLD) and other diseases.[15,16] It was also found that lower cardiovagal tone and BRS were negatively correlated with increased liver fat content in patients with type 2 diabetes.[17] Furthermore, the autonomic nervous system participates in the regulation of inflammation, oxidative stress, and the cardiovascular system.[8,9] Therefore, we speculate that the third possible pathological pattern of hepatic IR for promoting cardiovascular disease is autonomic dysfunction.

High-fat diet-induced some unfavorable outcomes, such as overweight, dyslipidemia, IR and hypertension, has been considered to be the main risk factors of cardiovascular diseases. Meanwhile, the development of IR, hypertension and atherosclerosis are affected by genetic and environmental factors. To our knowledge, whether hepatic IR promoting cardiovascular disorders that associated with low cardiovagal tone and BRS is true in minipigs, a more translationally-related large animal model remains unclear. Because of the similarity to a human in organ size, metabolism, cardiovascular system, and pathophysiological characteristics, pigs are examined the first choice for human studies in non-primate biomedical animal models.[18,19] In the comparison of genetic and environmental factors affecting humans and experimental animals, both genetic and environmental factors of minipigs are most similar to humans,[20] and genomic sequencing has confirmed that pigs are closer to humans than mice or rats,[21] which is critical to ensuring the transformative potential of animal studies. A high-fat diet is just an effective method to induce hepatic IR.[22] Our preliminary study found that Tibetan minipigs are an ideal model animal that studies the relationship between IR, metabolic syndrome and cardiovascular disease, and there is obvious autonomic dysfunction in the Tibetan minipig atherosclerosis model induced by HFC diet for 24 weeks.[23] Accordingly, we investigated hepatic IR (glycolipid metabolism, inflammation, insulin signaling pathway, and histopathology), autonomic function (HRV and BRS), and cardiac function in Tibetan minipigs model by using high fat/cholesterol (HFC) diet. We hypothesized that a long term HFC diet of Tibetan minipigs led to hepatic IR and promote cardiovascular disorders related to cardiovagal tone and baroreflex sensitivity (BRS) reduction.

2. Material and methods

2.1. Animal model

All animal husbandry, care, and experimental procedures were conducted in accordance with the Guide for the Care and Use of Laboratory Animals and were approved by the Institutional Animal Care and Use Committee of Zhejiang Chinese Medical University (ZSLL-2016-0031). Ten male Tibetan minipigs (Experimental Animal Center of Southern Medical University, Guangzhou, China) at 4 months of age, weighing 10–14 kg, were housed under temperature-controlled (20–22 °C) conditions with a 12: 12-h light-dark cycle. After adaptation to the environment for 4 weeks, minipigs were randomly divided into 2 groups: normal control (NC) and HFC. NC minipigs (n = 5) were fed a standard chow diet, contained protein, carbohydrates and fat, which accounted for 22%, 70% and 8% of the total calories, respectively, and had a caloric density of 3.39 kcal/g. HFC group (n = 5) were fed a diet of HFC chow containing a mixture of 1.5% cholesterol, 15% shortening oil, 10% egg yolk powder, and 73.5% regular chow. This mixture contained protein, carbohydrates and fat, which accounts for 19%, 50% and 31% of the total calories, respectively, and had a caloric density of 4.46 kcal/g. All minipigs in both groups received the same amount of food (2.5% of body weight) and were fed twice daily on a restricted schedule with a regular chow or HFC diet for 12 weeks until they were euthanized. Body mass index was calculated by anthropometric methods[24] and was defined as body weight (kg) divided by the square of the minipig length from the end of the snout to the base of the tail (m^2).

2.2. Determination of blood biochemical indices

Blood samples were collected from minipigs 16–18 h after fasting and then centrifuged (3000 rpm for 10 min at 4 °C) for serum collection. The levels of fasting blood glucose (FBG), total cholesterol (TC), low-density lipoprotein cholesterol (LDL-c), high-density lipoprotein cholesterol (HDL-c), and triglycerides (TG) in serum were determined using commercially available assays (Shanghai Shenneng-DiaSys Diagnostic Technology Co., Ltd., China) by an automatic biochemical analyzer (7020, HITACH, Japan). Atherogenic index (AI) was calculated using the formula: AI = (TC-HDL-c)/HDL-c. Serum nonesterified fatty acid (NEFA), insulin, and high-sensitive C-reactive protein (hs-CRP) concentrations were determined using commercially available ELISA kits (Nanjing Jiancheng Bioengineering Institute, China) as per manufacturer's instructions. The homeostasis models assessment of insulin resistance (HOMA-IR) was used as a surrogate measure of IR [(fasting insulin (mU/L) × fasting blood glucose (mg/dL)/405.1)]and the index of adipose tissue insulin resistance (AT-IR) was calculated using the formula: AT-IR = fasting insulin (mU/L) × fasting NEFAs (mg/dL).[25]

2.3. Intravenous glucose tolerance test (IVGTT)

At 12 weeks, each minipig was subjected to intravenous glucose tolerance test (IVGTT) as previously described.[23] A 22 G indwelling needle was inserted into the right ear vein to draw blood samples. The minipigs were injected with 50% glucose (0.5 g/kg) via an ear vein and finished within 2–3 min. Thereafter; the blood glucose and insulin

Table 1
Primers for quantitative real-time PCR analysis of gene expression.

Gene	Reverse primer	Forward primer	Product size
IRS1	GCAGGTGGATGATTCTGTGG	AGGAGGACTGGCTCTTGCTT	107
IRS2	CCTCCTTCCGTGGTGAACT	ATGCACTGTTGTGCTGTGTG	129
PI3K	GCAATGTGGAGCAGATGAAG	GGTAGAGCAGGAGGAAGTGG	108
Akt2	AAAGTCATCCTGGTGCG	GGGTGCCTGGTGTTCTG	137
Glut2	CATTCTTTGGTGGGATGCTT	ATGAGATGGTCCCAATTTCG	119
mTOR	CTTTGTCCAGACCATGCAGCAGC	TCGTTGATGCCCTGTAGGTTCAGCT	141
GSK3β	GCTTCAACCCCTTCAAATGC	GACGCAGAAGCGGTGTTATTG	133
PGC1α	GTGTCGCCTTCTTGTTCTTCTTTT	CGCATCCTTTGGGGTCTTT	92
TNF-α	CCACGCTCTTCTGCCTACTGC	CTCGGCTTTGACATTGGCTAC	161
FOXO1	TGTCCTACGCCGACCTCAT	TTGCTGTC ACCCTTATCCTTG	124
PEPCK	CAGTGCCATGCGCTCAGAGTC	CCATGCTCAGCCAGTGTTCCAG	131
G6PC	ATCTACAACGCCAGCCTCAAGAAG	CCGCTCACACCTTCGCTTGG	141
GAPDH	CCATCACCATCTTCCAGGAGCGAG	AAGTTGTCATGGATGACCTTGGCCA	286

IRS1: insulin receptor substrate 1; *IRS2*: insulin receptor substrate 2; *PI3K*, phosphatidylinositol 3-kinase, *Akt 2*: alanine aminotransferase assav 2; *Glut2*: glucose transporter type 2; *mTOR*: mammalian target of rapamycin; *GSK3β*: glycogen synthase kinase-3β; *PGC1α*: peroxisome proliferator-activated receptor gamma coactivator 1-alpha; *TNF-α*: tumor necrosis factor alpha; *FOXO1*: Forkhead box O1; *PEPCK*: phosphoenolpyruvate carboxykinase; G6PC: glucose-6-phosphatase; GAPDH: glyceraldehyde-3-phosphate dehydrogenase.

concentrations were measured after 0, 5, 15, 30, 60, 90, and 120 min. Glucose and insulin area under curves (AUC) from the baseline were calculated. Moreover, the insulin sensitivity index (S2) derived from IVGTT was calculated as previously described.[26]

2.4. Liver triglycerides, MDA and NEFA content measurements

Liver triglycerides content was determined using a commercially available kit (Shanghai Shenneng-DiaSys Diagnostic Technology Co., Ltd., China). Briefly, the liver tissue (100–200 mg) was homogenized in 4 mL of isopropanol for 7–10 min, and then the homogenate was centrifuged at 4600 rpm for 10 min, and a microplate spectrophotometer (Thermo Varioskan Flash, Thermo Fisher, Finland) was used to analyze the absorbance set at a wavelength of 582 nm. Data are expressed as mg/g wet weight liver, as previously described.[27] The malondialdehyde (MDA) content was examined with sulfur barbiturate acid method.[28] Fresh liver tissues were made into 10% homogenate for measurement of MDA and NEFA content. MDA and NEFA content was determined using a commercially available kit (Nanjing Jiancheng Bioengineering Institute, China). The liver protein concentration of all samples was determined by the Coomassie brilliant blue method, and the MDA and NEFA contents were normalized to the total protein content of the sample.

2.5. Blood pressure measurement

The blood pressure was continually recorded by the tail-cuff method with a non-invasive physiological signal telemetry system (EMKA Technologies S.A.S., France) as previously described.[23] The systolic blood pressure (SBP), diastolic blood pressure (DBP) and Mean blood pressure (MBP) were analyzed by ECGAUTO software (EMKA Technologies S.A.S., France).

2.6. HRV analysis

At 12 weeks, the physiological telemetry test and HRV analysis were performed for each minipig as previously described.[23,29] Briefly, ECG electrodes were connected and Lead II ECG was monitored for 3 h and recorded using a non-invasive physiological signal telemetry system (EMKA Technologies S.A.S., France). HRV analysis was made using the HRV analysis module of ECG-Auto software (EMKA Technologies S.A.S., France). The time domain indices (TDIs) such as mean RR interval (RRI), standard deviation of all RRIs (SDNN), and square root of the mean square successive differences between successive normal intervals (RMSSD), and frequency domain indices (FDIs) such as total power (TP), low frequency (LF) component expressed as normalized

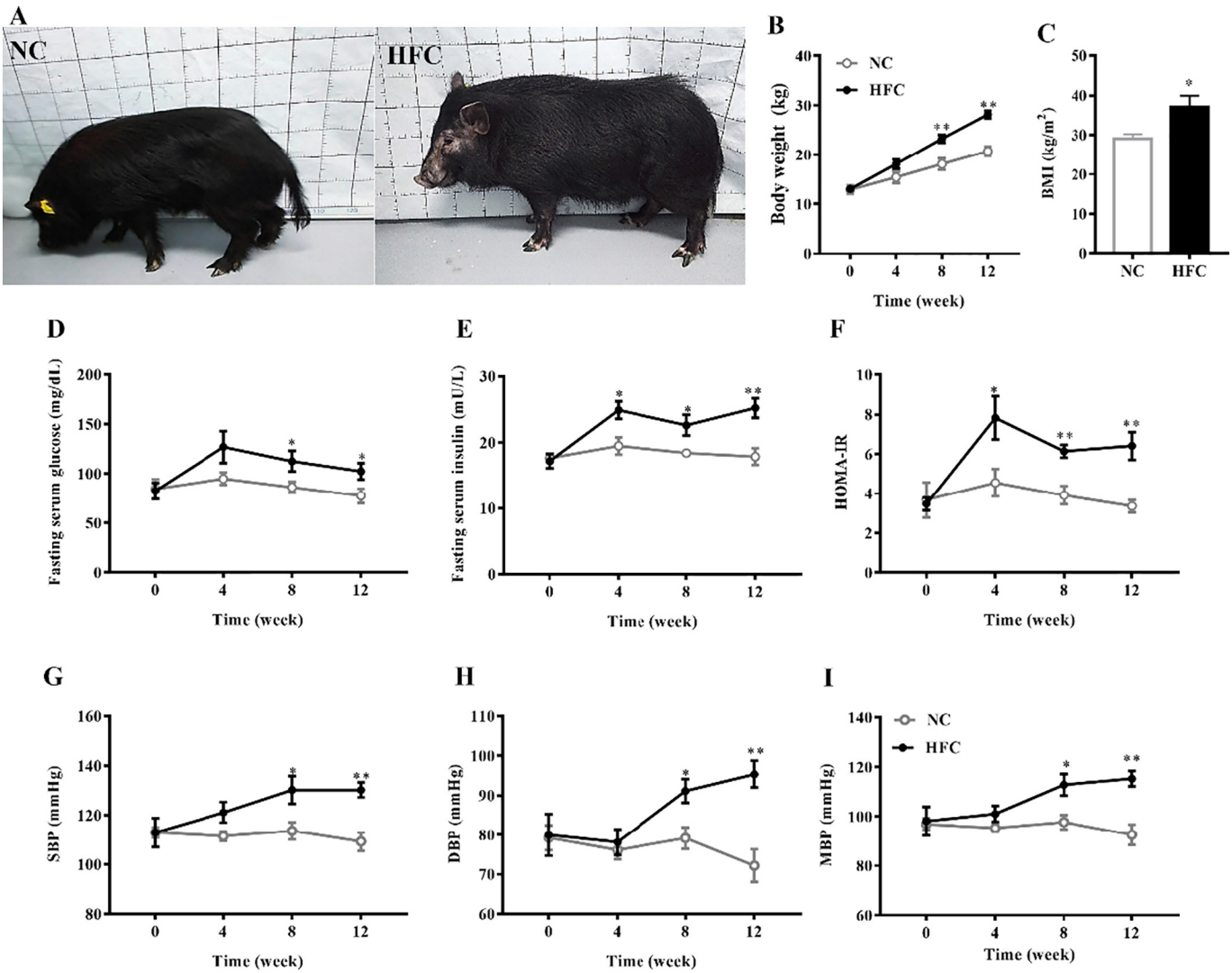

Fig. 1. Gross appearance, fasting blood glucose, insulin levels, HOMA-IR, and blood pressure results in Tibetan minipigs. Minipigs were fed with normal control (NC) or HFC diets for 12 weeks. (A) At 12 weeks, HFC-fed minipigs were obese, had thicker abdominal fat, and back fat compares to NC diet minipigs. (B) Body weight, (C) body mass index (BMI), (D) fasting blood glucose, (E) fasting insulin, (F) HOMA-IR, (G) systolic blood pressure(SBP), (H) diastolic blood pressure (DBP), (I) mean blood pressure (MBP). Data are expressed as means ± SEM (n = 5). $^{*}P < 0.05$, $^{**}P < 0.01$ versus NC group.

Table 2
The effects of HFC diet on lipid profile, insulin-related profile, and inflammatory markers in Tibetan minipigs after 12-week feeding.

Parameters	NC diet	HFC diet
Lipid profile and lipid risk factors		
TC (mg/dL)	69.14 ± 7.20	585.46 ± 60.01**
TG (mg/dL)	17.05 ± 1.67	18.38 ± 3.22
HDL-c (mg/dL)	24.59 ± 1.97	115.55 ± 5.20**
LDL-c (mg/dL)	24.44 ± 1.97	389.25 ± 45.78**
AI	1.85 ± 0.35	4.07 ± 0.44**
Insulin-related parameters		
FBG (mg/dL)	77.58 ± 7.29	107.01 ± 8.55*
Insulin (mU/L)	17.87 ± 1.26	25.23 ± 1.49**
NEFA (mg/dL)	0.38 ± 0.02	1.28 ± 0.29**
HOMA-IR	3.36 ± 0.16	6.42 ± 0.70**
AT-IR	6.54 ± 0.34	31.28 ± 5.73*
Inflammatory marker		
hs-CRP(mg/L)	5.87 ± 1.26	16.62 ± 2.82*

All minipigs were fasted 16–18 h before taking blood samples. NC: normal control diet; HFC: high fat/cholesterol diet; TC: total cholesterol; TG: triglycerides; HDL-c: high density lipoprotein-cholesterol; LDL-c: Low density lipoprotein-cholesterol; FBG: fasting blood glucose; NEFA: non-esterified fatty acids; HOMA-IR: homeostatic model assessment of insulin resistance; AT-IR: index of adipose tissue insulin resistance; hs-CRP: high sensitive C-reactive protein. Data are expressed as means ± SEM (n = 5). $^{*}P < 0.05$, $^{**}P < 0.01$ versus NC group.

unit (LFnu), high frequency (HF) component expressed as normalized unit (HFnu), and LF/HF ratio were recorded.

2.7. Cardiac function and baroreflex sensitivity (BRS) assessments

On the last day of protocol, each minipig was anesthetized by inhalation of 2–3% isoflurane-oxygen mixture delivered by a mask and then intubated, maintained anesthesia with 0.5–2% isoflurane-oxygen mixture. During anesthesia, minipigs were placed on heating pads maintained at 37 °C and monitored for body temperature and ECG (Life Window 6000; Digicare Animal Health, Boynton Beach, FL, USA). Each minipig was implanted with three saline-filled (heparinized 50 IU/mL) catheters. One catheter was inserted into the left ventricle (LV) via right carotid artery to record the cardiac function parameters [(left ventricular systolic pressure (LVSP), left ventricular end diastolic pressure (LVEDP), the maximum rise rate of left ventricular pressure (LV +dp/dtmax) and the maximum fall rate of left ventricular pressure (LV −dp/dtmax)], the second catheter was inserted into the left femoral artery to record systolic blood pressure (SBP) and beat interval (BI), the third catheter was inserted into the right ear vein to administrate a drug. All signals were constantly recorded by using a non-invasive physiological signal telemetry system (EMKA Technologies S.A.S., France).

Baroreflex sensitivity (i.e., change in BI/change in SBP) in response to phenylephrine (PE) and sodium nitroprusside (SNP) injections were tested as previously described.[30] Phenylephrine (PE, Aladdin industrial corporation, Shanghai, China), an alpha stimulant vasoconstrictor, was administered at a dose of 3, 6, and 12 μg/kg (120 μg/mL). Sodium nitroprusside (SNP, Wuhan Humanwell Pharmaceutical Co., Ltd., China), a direct-acting vasodilator, was administered at a dose of 2.5, 5, and 10 μg/kg (100 μg/mL). The second administration should be administered when the previous BI and SBP reactions reach a steady state.

2.8. Total RNA isolation and Real time-PCR

Total RNA was extracted from liver samples using TAKARA RNAiso plus reagent (TAKARA, Japan) according to the instructions. Determination of RNA content, mRNA quantification, and real-time polymerase

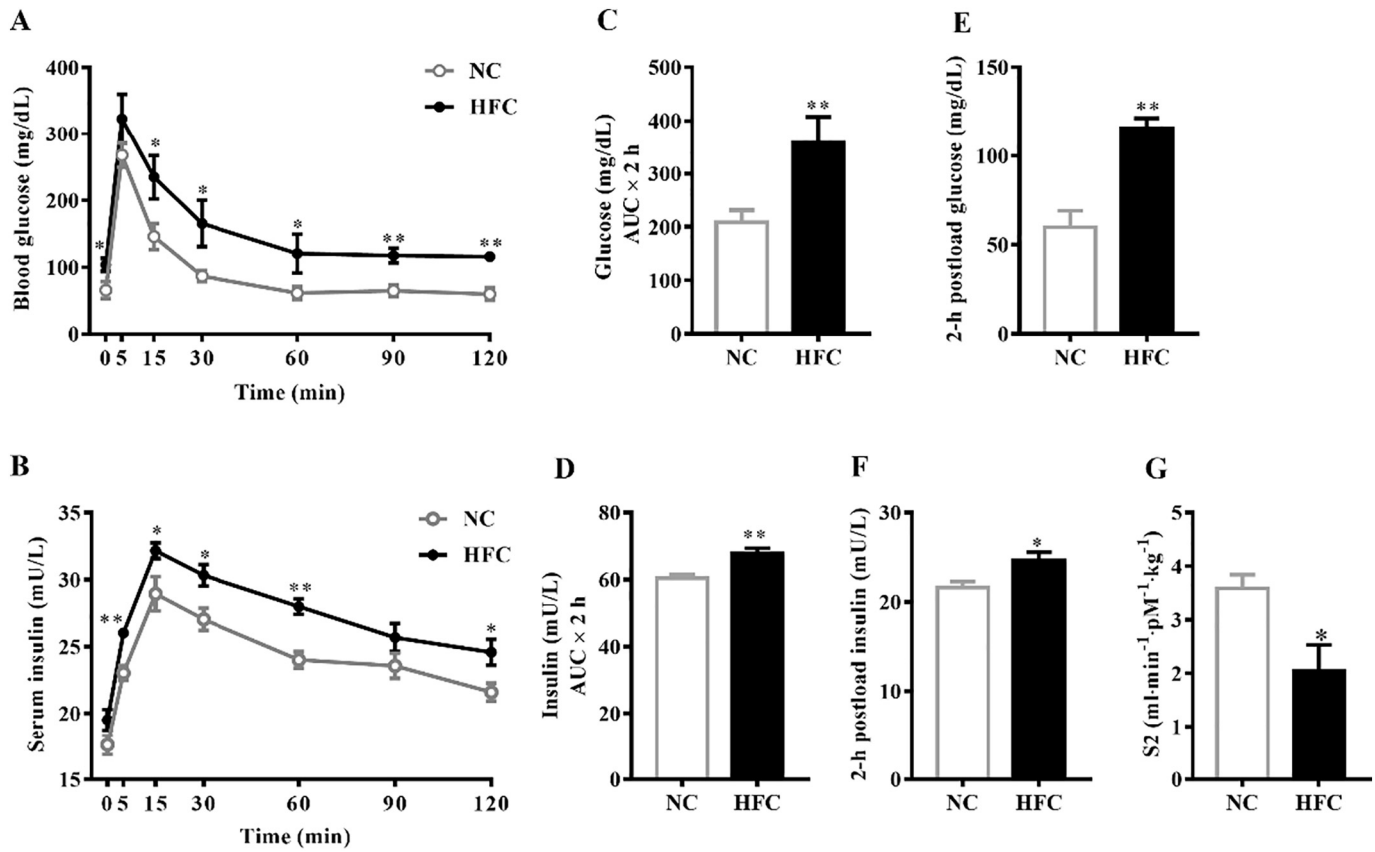

Fig. 2. Glucose and insulin response to intravenous glucose tolerance test (IVGTT) in NC and HFC diet fed minipigs. All minipigs were subjected to IVGTT at 12-week time points. Briefly, the fasting minipigs were injected with a glucose solution of 0.5 g/kg body weight via the jugular vein. For analyzing IVGTT results, the glucose (A) and insulin secretory response (B) during IVGTT, the area under the curve (AUC) of glucose (C) and insulin (D) levels, 2-h postload glucose (E) and insulin (F) levels, and insulin sensitivity index (S2) (G) are shown. Data are expressed as means ± SEM (n = 5). $^{*}P < 0.05$, $^{**}P < 0.01$ versus NC group.

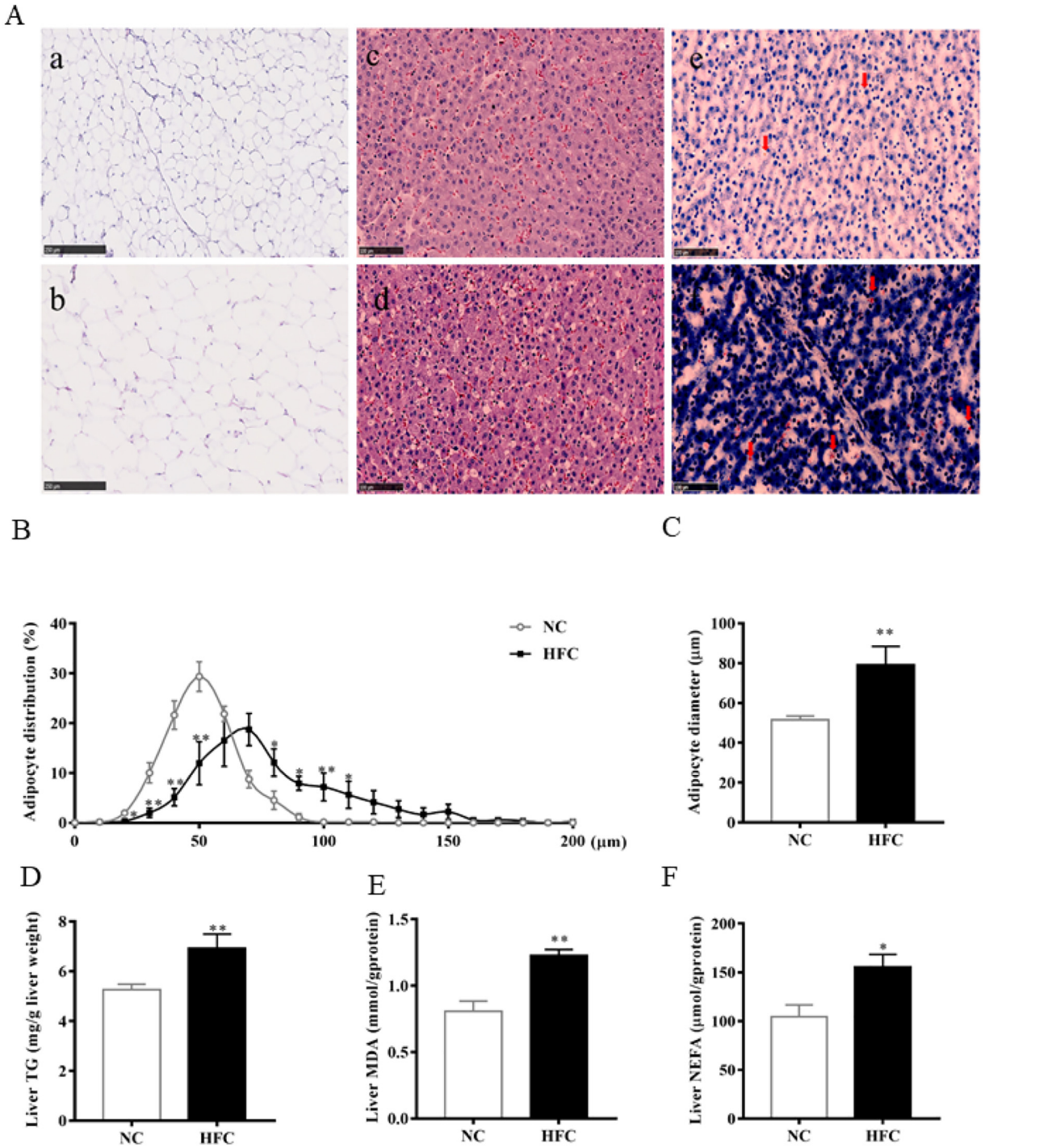

Fig. 3. Histopathological assessments and the changes of liver TG, MDA, and NEFA contents in NC and HFC diet fed minipigs. Representative micrographs of adipose tissue (H&E, a, b), liver tissue (H&E, c, d) and Oil Red O staining (e, f) in liver tissue are shown (A). Adipocyte cells size distribution (B) and mean diameter (C) in visceral fat was calculated. The contents of TG (D), MDA (E) and NEFA (F) in liver tissue. The red arrow indicates lipid deposition. Data are expressed as means ± SEM (n = 5). $^{*}P < 0.05$, $^{**}P < 0.01$ versus NC group.

chain reaction (IQ5 RT-PCR; Bio-Rad, Richmond, CA, USA) were performed according to previously described.[23] The primer sequences for the target and reference genes (IRS1, IRS2, PI3K, Akt2, Glut2, mTOR, GSK-3β, PGC1α, TNF-α, FOXO1, PEPCK, G6PC and GAPDH) used for real-time PCR are listed in Table 1. Briefly, a reaction system of 20 μL was composed of 10 μL of SYBR Premix Ex Taq (TAKARA, Japan), 1 μL of forward primer, 1 μL of reverse primer, 0.4 μL ROX Reference Dye, 5.6 μL of DEPC-treated water, and 2 μL of complementary DNA. The $2^{-\Delta\Delta Ct}$ method was used to calculate relative expression values.

2.9. Liver protein extraction and Simple Western analysis

Liver protein was extracted according to manufacturer protocols provided by the extraction kit (KeyGen BioTech, Nanjing, China). Protein levels were determined by capillary electrophoresis size-based separating via Wes from Protein Simple according to the manufacturer instructions. Protein identification and quantification were analyzed with Compass software (ProteinSimple, USA). Antibodies used for Simple Western included anti-IRS-1 (H-7; Santa Cruz Biotechnology; sc-

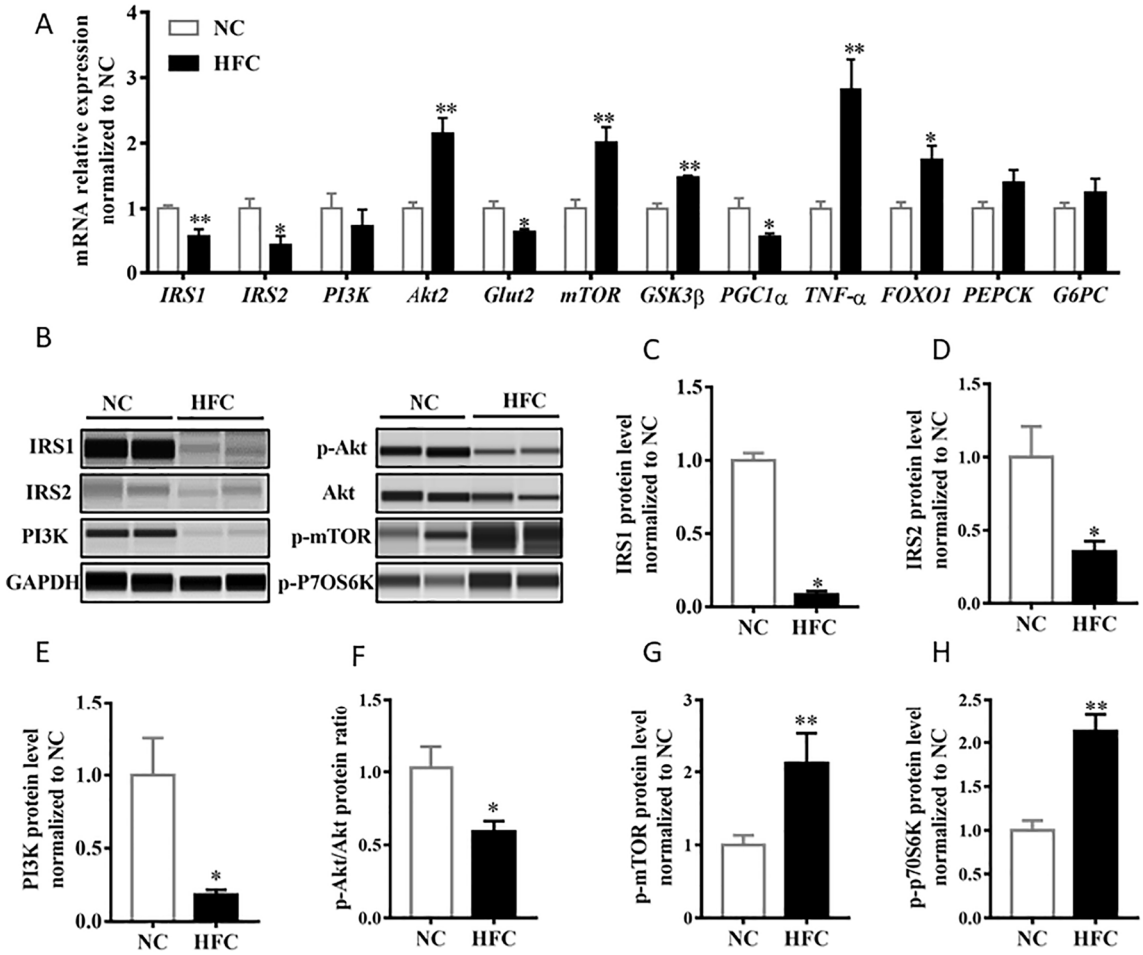

Fig. 4. Gene expressions and protein levels of liver tissue in NC and HFC diet fed minipigs. (A) The changes of *IRS2*, *PI3K*, *Akt2*, *Glut2*, *mTOR*, *GSK3β*, *PGC1α*, *TNF-α*, *FOXO1*, *PEPCK*, and *G6PC* mRNA expression in liver tissue. (B) Protein bands of IRS1, IRS2,PI3K, p-Akt, Akt, p-mTOR, p-P7OS6K proteins in liver tissue by Wes, and quantification of (C) IRS1, (D) IRS2, (E) PI3K, (F) p-Akt/Akt, (G) p-mTOR and (H) p-p70S6K proteins. Data are expressed as means ± SEM (n = 5). $^{*}P < 0.05$, $^{**}P < 0.01$ versus NC group.

515017,1:50), anti-IRS-2 (B-5; Santa Cruz Biotechnology; sc-390761,1:50), anti-PI3K p110 (B-5; Santa Cruz Biotechnology; sc-e76412,1:50), anti-phospho-AKT (Ser 473; Cell Signaling Technology; #4060, 1:50), anti-pan-AKT (C67E7; Cell Signaling Technology; #4691,1:50), anti-phospho-mTOR (Ser 2448; Santa Cruz Biotechnology; sc-293133,1:50), and anti-phospho-p70S6K (E-5; Santa Cruz Biotechnology; sc-377529,1:50). All proteins were normalized to GAPDH (Santa Cruz Biotechnology; sc-166545, 1:100).

2.10. Pathological examination

Upon anesthesia at 12 weeks, the chest of each minipig was opened to achieve euthanasia. Samples of liver and adipose tissues were removed from each animal, and then these materials were disposed of as follows: 10% phosphate-buffered formalin-fixed, dehydrated, and embedded in paraffin and then cut into 4-μm-thick slices. Then slices were analyzed with hematoxylin & eosin (H&E) staining. In addition, fresh liver tissues were embedded in optimum cutting temperature compound (OCT) and cryosectioned. The slices were fixed in 4% paraformaldehyde in PBS and were stained with 0.5% Oil Red O (Sigma-Aldrich, St. Louis, MO) according to the standard procedure as previously described.[31] All sections were scanned with a Hamamatsu Skeleton Scanner (Nanozoomer S210, Hamamatsu, Japan). Adipocyte cell size distribution and mean diameter in visceral fat were calculated by Image-pro-plus 6.0 software.

2.11. Statistical analysis

All results are expressed as means ± SEM. SPSS 20.0 software (SPSS, Chicago, IL, USA) was used to perform statistical analysis. Data were compared using Student's *t*-test. Correlation analysis was done with Pearson's test followed by multiple linear regression analysis. A two-tailed $P < 0.05$ was considered statistically significant.

3. Results

3.1. Monthly body weight, fasting blood glucose and insulin levels, and blood pressure

Tibetan minipigs fed the HFC diet gained weight more rapidly at 8 weeks and 12 weeks than that fed with NC diet ($P < 0.01$) (Fig. 1A and B).The BMI of the HFC group significantly increased during the 12th week ($P < 0.05$, Fig. 1C). The fasting blood glucose in the HFC-fed minipigs was significantly increased at 8 and 12 weeks of the experiment ($P < 0.05$, Fig. 1D). Meanwhile, the fasting insulin and HOMA-IR in the HFC-fed minipigs were gradually increased during the 4-week feeding period ($P < 0.05$, $P < 0.01$, Fig. 1E and F). In addition, the MBP, SBP, and DBP in the HFC-fed minipigs were significantly increased at 8 weeks and 12 weeks ($P < 0.05$, $P < 0.01$, Fig. 1G–I).

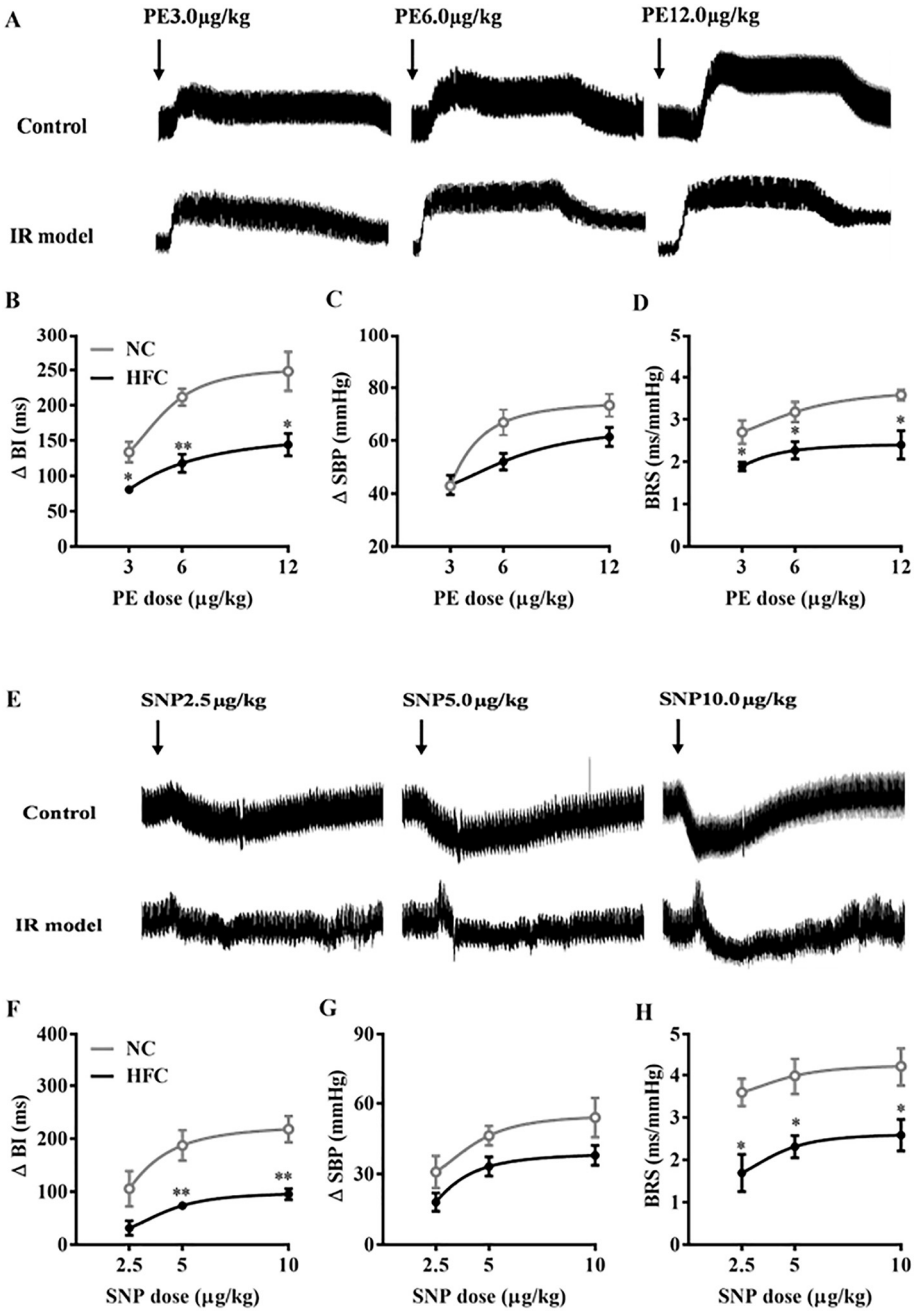

Fig. 5. Changes of baroreflex sensitivity in NC and HFC diet fed minipigs following phenylephrine (PE) or sodium nitroprusside (SNP) administration. (A) Traces of blood pressure changes induced by PE application at 3, 6 and 12 μg/kg. (B) The curve of change in beat interval (△BI) against each of PE. (C) The curve of change in systolic blood pressure (△SBP) against each of PE. (D) The curve of BRS against different doses of PE. (E) Traces of blood pressure changes induced by SNP application for 2.5, 5 and 10 μg/kg. (F) The curve of change in beat interval (△BI) against each of SNP. (G) The curve of change in systolic blood pressure (△SBP) against each of SNP. (H) The curve of BRS against different doses of SNP. Data are expressed as means ± SEM (n = 5). *$P < 0.05$, **$P < 0.01$ versus NC group.

3.2. Serum biochemical profiles

At 12 weeks, all lipid profile and AI were significantly increased in the HFC group compared to the NC group ($P < 0.01$, Table 2), except for TG. FBG, insulin, NEFA, HOMA-IR, and AT-IR were substantially increased in the HFC group compared to the NC group ($P < 0.05$, $P < 0.01$, Table 2). Similarly, the hs-CRP level was significantly increased in the HFC group compared to the NC group ($P < 0.05$, Table 2).

3.3. Intravascular glucose tolerance test (IVGTT)

To investigate whether the HFC diet led to impaired glucose clearance and insulin sensitivity, an IVGTT trial was conducted at 12 weeks. The IVGTT showed that HFC-fed minipigs had significantly higher blood glucose and insulin secretory after 0.5 mg/kg glucose administration ($P < 0.05$, $P < 0.01$, Fig. 2A–D). 2 h-postload glucose and 2 h-postload insulin were increased substantially in the HFC group compared to the NC group ($P < 0.05$, $P < 0.01$, Fig. 2E and F). In contrast, the S2 was drastically decreased in the HFC group compared to the NC group ($P < 0.05$, Fig. 2G).

3.4. Pathological examinations and liver TG, MDA, and NEFA contents measurement

To investigate the pathological changes induced by the HFC diet, we examined the pathological changes in the adipose and liver tissue.

Table 3
HRV indices and cardiac function parameters of NC diet and HFC diet groups.

Parameters	NC diet	HFC diet
FDI of HRV		
TP (ms^2)	920.7 ± 144.8	280.1 ± 88.9**
LFnu	25.24 ± 3.45	67.72 ± 6.06**
HFnu	74.76 ± 3.45	32.28 ± 6.06**
LF:HF	0.35 ± 0.06	2.59 ± 0.67*
TDI of HRV		
Mean RRI (ms)	477.4 ± 45.5	424.4 ± 70.2
SDNN (ms)	72.91 ± 3.12	47.17 ± 8.77*
RMSSD (ms)	59.85 ± 3.97	23.66 ± 10.76*
Cardiac function parameters		
LVSP (mm Hg)	128.9 ± 12.7	118.7 ± 10.5
LVEDP (mm Hg)	0.83 ± 1.54	8.60 ± 2.60*
LV +dp/dtmax (mm Hg/s)	2336.9 ± 345.8	1074.5 ± 86.4*
LV −dp/dtmax (mm Hg/s)	−2134.4 ± 240.0	−1063.1 ± 101.2**

The values are expressed as means ± SEM, n = 5. *$P < 0.05$, **$P < 0.01$ versus NC group. HRV: heart rate variability, FDI: frequency domain indices of HRV, TP: total power, LFnu: normalized low frequency component; HFnu: normalized high frequency component; LF: HF: ratio of low frequency component to the high frequency component of HRV; TDI: time domain indices of HRV; Mean RRI: mean-RR interval; SDNN: standard deviation of all normal RR intervals; RMSSD: square root of the mean square successive differences between successive normal intervals. LV: left ventricle; LVSP: left ventricular systolic pressure, LVEDP: left ventricular end diastolic pressure; LV +dp/dtmax: the maximum rise rate of left ventricular pressure; LV −dp/dtmax: the maximum fall rate of left ventricular pressure.

Analysis of adipocyte size showed that the average adipocyte was larger in HFC-fed minipigs compared to NC-fed minipigs (Fig. 3A–a, and b), and the adipose of HFC group was shifted toward a large cell population compared with NC group ($P < 0.05$, $P < 0.01$, Fig. 3B and C). Histological analysis showed significant hepatic steatosis in HFC group by H&E staining (Fig. 1A–c, and d), and oil red O staining also confirmed significant lipid deposition in HFC group (Fig. 3A–e, and f). Moreover, the biochemical analysis also showed that liver TG, MDA, and NEFA contents were significantly increased in HFC-fed minipigs ($P < 0.05$, $P < 0.01$, Fig. 3D, E and F).

3.5. Impairment of hepatic insulin signaling pathway in HFC-fed minipigs

To investigate the effects of the HFC diet on hepatic insulin signaling, the related genes and proteins expression were evaluated. As shown in Fig. 4, feeding an HFC diet to minipigs significantly suppressed mRNA expression of *IRS1*, *IRS2*, *Glut2*, and *PGC1α* ($P < 0.05$, $P < 0.01$), and increased mRNA expression of *Akt2*, *mTOR*, *GSK3β*, *TNF-α*, and *FOXO* in liver tissue ($P < 0.05$, $P < 0.01$). However, there were no significant differences in liver *PI3K*, *PEPCK*, and *G6PC* mRNA expression between both groups ($P > 0.05$). In addition, HFC-fed minipigs had significantly decreased protein levels of liver IRS1, IRS2, PI3K, and p-Akt/Akt ($P < 0.05$), as well as markedly increased the protein levels of liver p-mTOR and p-p70S6K ($P < 0.01$).

3.6. Lower baroreflex sensitivity in HFC-fed minipigs

To investigate the baroreflex sensitivity of HFC-fed minipigs, the baroreflex sensitivity of PE or SNP-induced blood pressure changes in all minipigs was determined. As shown in Fig. 5, the effects of PE and SNP on blood pressure changes in opposite directions, these data reflect the relationship between blood pressure and beat interval, i.e., the baroreflex response. Compared with the NC group, the ΔBI and BRS values of the HFC group induced by 3–12 μg/kg PE were significantly decreased ($P < 0.05$, $P < 0.01$). Similarity, the ΔBI and BRS values of the HFC group induced by 5–10 μg/kg and 2.5–10 μg/kg SNP, were significantly decreased ($P < 0.01$, and $P < 0.05$, respectively). However, the ΔSBP response induced by PE or SNP in HFC-fed minipigs showed a weakening tendency, but the difference was not significant ($P > 0.05$).

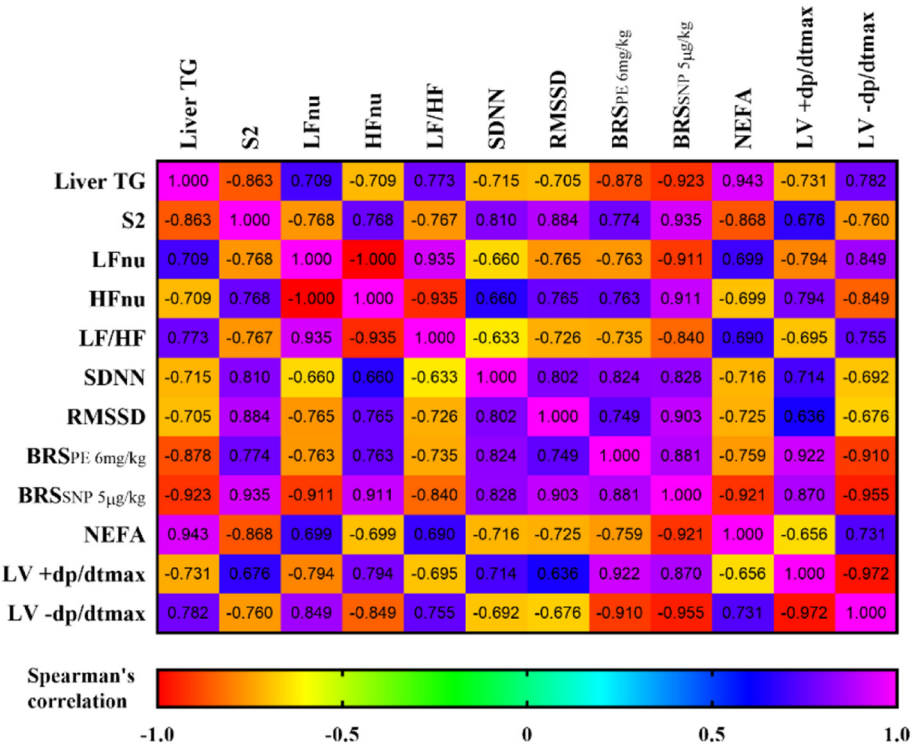

Fig. 6. Correlation analyses among hepatic IR, autonomic function and cardiac function. Liver TG content was positively correlated with LFnu, LF/HF, NEFA, and LV −dp/dtmax, and negatively correlated with HFnu, SDNN, RMSSD, BRS, S2 and LV +dp/dtmax.

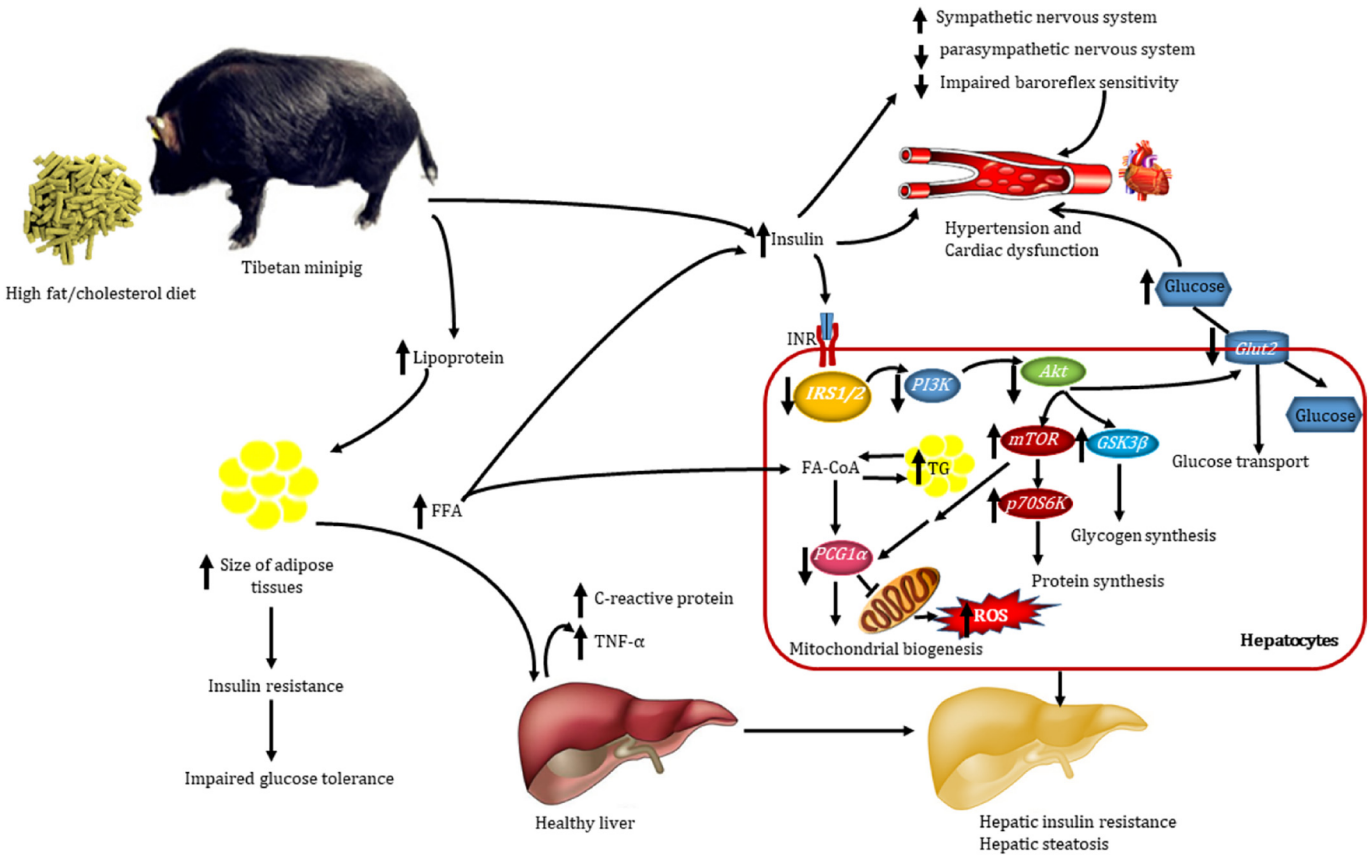

Fig. 7. Schematic representation of lower cardiovagal tone and BRS are associated with hepatic IR and promote cardiovascular disorders in Tibetan minipig induced by high fat/cholesterol (HFC) diet. (1) HFC diet leads to obesity, hyperglycemia, hyperinsulinemia, dyslipidemia, glucose intolerance, inflammatory, and peripheral insulin resistance. (2) HFC diet leads to expand adipose tissues, and FFA are released in abundance from an expanded adipose tissue mass. In the liver, FFA result in increased production of glucose and triglycerides, FFA simultaneously reduce hepatic insulin sensitivity by inhibiting insulin signaling pathway (IRS/PI3K/AKT) and affect downstream signaling molecule (such as Glut2, GSK3β, mTOR and PGC-1α), causing disorders of glycolipid metabolism, resulting in hepatic IR, hepatic steatosis and elevated fasting hyperglycemia, and with the body oxidative stress and inflammation reaction, promote the activity of sympathetic nervous system, parasympathetic activity and BRS decreased, cause cardiovascular dysfunction.

3.7. Depressed HRV and cardiac dysfunction in HFC-fed minipigs

Among the frequency domain indices of HRV, TP and HFnu were significantly decreased ($P < 0.01$), LFnu and LF/HF ratio were significantly increased ($P < 0.05$, $P < 0.01$) in HFC group compared to the NC group (Table 3). Meanwhile, Time domain indices of HRV (SDNN and RMSSD) were substantially decreased ($P < 0.05$) in the HFC group compared to the NC group (Table 3). Cardiac function parameters such as LVSP ($P > 0.05$), LV +dp/dtmax ($P < 0.05$), and LV −dp/dtmax ($P < 0.01$) were either slight or significantly decreased except the LVEDP ($P < 0.05$), which was found to be significantly increased in the HFC group compared to the NC group (Table 3).

3.8. Correlation analyses among hepatic IR, autonomic function and cardiac function

As shown in Fig. 6, the correlation analysis showed that liver TG content was positively correlated with LFnu ($r = 0.709$, $P < 0.05$), LF/HF ($r = 0.773$, $P < 0.01$),NEFA ($r = 0.943$, $P < 0.01$), and LV −dp/dtmax ($r = 0.782$, $P < 0.01$) and negatively correlated with HFnu ($r = -0.709$, $P < 0.05$), SDNN ($r = -0.715$, $P < 0.05$), RMSSD ($r = -0.705$, $P < 0.05$), BRS ($r_{PE\ 6\mu g/kg} = -0.878$, $P < 0.01$ and $r_{SNP\ 5\mu g/kg} = -0.923$, $P < 0.01$), S2 ($r = -0.863$, $P < 0.01$), and LV +dp/dtmax ($r = -0.731$, $P < 0.05$). In addition, further multiple linear regression analysis shows that $S2 = -1.733 + 0.075\ HFnu + 0.039\ RMSSD + 3.681\ BRS_{PE\ 6\mu g/kg} - 2.774\ BRS_{SNP\ 5\mu g/kg} - 4.931\ NEFA + 1.146$ liver TG + 0.003 LV −dp/dtmax.

4. Discussion

In this study, we explored the relationship among HFC diet-induced autonomic dysfunction, hepatic IR and cardiovascular disorders in Tibetan minipigs. According to the results, the HFC-fed minipigs presented several characteristics similar to IR subjects, including obesity, dyslipidemia, hyperglycemia, hyperinsulinemia, and hypertension.[32] Glucose intolerance and impaired hepatic insulin signal transduction, which could lead to hepatic IR, were also displayed in minipigs. In addition, the levels of hs-CRP and TNF-α were also increased in HFC-fed minipigs, indicating that IR is associated with obesity, increased fat, and inflammation. Moreover, there were obvious left ventricular diastolic dysfunction and early features of sympathovagal imbalance, such as decreased HRV and BRS. The multiple linear regression analysis indicated that hepatic IR toward cardiovascular disease was associated with low HFnu, RMSSD, BRS and LV −dp/dtmax, high NEFA, high hepatic TG content. All of these changes suggested that the HFC diet can result in hepatic IR and promote cardiovascular disorders, associated with lower cardiovagal tone and BRS. Therefore, the minipig model may contribute to understanding the relationship between hepatic IR and cardiovascular diseases in human (Fig. 7).

Changes in visceral fat content can alter insulin sensitivity and IR.[33] The HOMA-IR index provides a reasonable assessment of IR both in animals and humans,[34] and the IVGTT-derived S2 index is more sensitive to evaluate insulin sensitivity that has been proved to correlate with hyperinsulinnormal glucose clamp test in pigs.[26] In this study, HFC diet-induced minipigs had obvious signs of peripheral IR signs, such as fasting hyperglycemia, hyperinsulinemia, increased HOMA-IR index, increased area under

curves of glucose and insulin levels after IVGTT, as well as a decreased S2 index. In addition, IR is linked to ectopic lipid deposition caused by lipotoxicity. Gastaldelli et al[35] revealed that the negative correlation with peripheral insulin sensitivity was greater with intrahepatic fat than that with visceral fat. Similarly, we observed that intrahepatic fat is significantly negatively correlated with the S2 index in HFC-fed minipigs. However, how intrahepatic fat causes IR and independent of visceral fat are still unclear. Some studies have indicated that FFA is an important link between lipid metabolism disorders and IR or hyperinsulinemia. Excessive FFAs in blood deposit in the liver in the form of triglycerides, which result in hepatic IR.[36] On the other hand, FFA-induced oxidative stress, another important cause of hepatic IR, can induce hepatic inflammation and glycolipids metabolic disorders.[37] Our results confirm that FFA-induced ectopic lipid deposition and oxidative stresses are involved in the development of hepatic IR in HFC-fed minipigs. In addition, hepatic chronic inflammation caused by fat accumulation can enhance various inflammatory mediators such as interleukin and tumor necrosis factor (TNF), and cause hepatic IR. Overexpression of TNF-α can cause an increase in CRP synthesis in the liver and aggravate IR by inhibiting insulin receptor tyrosine kinase activity.[38] In this study, hs-CRP and TNF-α levels in HFC-fed minipigs were significantly elevated, indicating that hepatic chronic inflammation was associated with IR.[39]

Lipid accumulation in hepatocytes affects the structure and function of the cell surface and the physiological effects of hepatic insulin mainly depend on the IRS/PI3K/AKT signaling pathway to play its part.[40] When insulin binds to its receptor, the insulin receptor is activated by autophosphorylation and further acts on tyrosine residues of the downstream IRS. Tyrosine-phosphorylated IRS binds to PI3K's SH2, thereby activating the downstream PI3K-PIP3 signaling pathway and further inducing Akt phosphorylating via PDK1. Activated Akt exerts metabolic regulation of glucose and fat by acting on downstream Glut2, GSK3β, mTOR and PGC-1α. Thus, PI3K/Akt signaling pathway, one of the insulin signaling pathways, plays a major role in glucose transport, glycogen synthesis, glycolysis, and gluconeogenesis as well as protein synthesis and lipolysis process.[41] In this study, decreased IRS1, IRS2, PI3K activities and phosphorylation level of Akt were observed in liver tissues of HFC-fed minipigs, indicating that attenuated IRS/PI3K/Akt signaling pathway was one of the main mechanisms of hepatic IR in HFC-fed minipigs, which was consistent with previous results.[42,43] Recently, it has been observed that high expression of GSK-3β is associated with decreased insulin sensitivity. Impaired glucose tolerance and elevated insulin levels were represented in GSK-3β transgenic male mice.[44] Glut2 plays an important role in insulin-activated glucose uptake in liver, and inhibition of glucose release from hepatocytes. Increased expression of GSK-3β and decreased expression of Glut2 in the liver tissues of HFC-fed minipigs indicated that Glut2 translocation is blocked due to the decreased phosphorylation level of Akt, which would result in promoting the expression of gluconeogenesis genes (such as FOXO1), accompanied by the increased gluconeogenesis and the impairment of glycogen synthesis,[45] and finally leads to fasting hyperglycemia.

The mTOR/p70S6K pathway mainly regulates cell growth and protein synthesis. mTOR/p70S6K may be overexpressed for a long time under long-term stimulation of high concentration glucose, causes excessive phosphorylation of IRS-1 serine/threonine, hinders the phosphorylation of its tyrosine, further inhibits the PI3K/Akt signal transduction and makes the PI3K/Akt pathway inactivation, ultimately leading to IR.[46,47] Moreover, activation of mTOR/p70S6K pathways may also result in decreased PGC-1α activity. Thereby resulting in a decline in nutrients oxidative metabolism and mitochondrial dysfunction, which in turn cause IR and obesity.[48] In this study, HFC diet-induced the activation of the mTOR/p7Os6K signaling pathway and decreased expression of PGC-1α in the liver of minipigs, which was similar to the results of human and animal studies.[49,50]

Previous studies have confirmed that hepatic IR could directly or indirectly promote the occurrence of cardiovascular disease, which was linked to the changes in body composition, dyslipidemia, and low-grade inflammation.[6] Interestingly, autonomic dysfunction was also found to be involved in the hepatic IR promoting cardiovascular disorders in HFC-fed minipigs, such as the increased LF/HF ratio and LFnu, indicating sympathovagal imbalance and sympathetic tone activation,[51] as well as reduced RMSSD, HFnu and BRS, showing a lower cardiovagal tone.[52,53] In fact, the liver is also dominated via the sympathetic nervous system and the parasympathetic nervous system, which are derived from the portal vein, the hepatic artery and the visceral and vagal nerve around the bile duct. The balanced autonomic output of the liver is important for maintaining the circadian rhythm of metabolic enzymes and glucose levels in the liver.[54] It has been observed that vagal denervation significantly elevates triglycerides level,[55] whereas the preservation of vagal activity played a protective role in the hepatic fat accumulation in patients with type 2 diabetic.[17] Rattarasarn C et al[56] found a positive correlation between intrahepatic fat and IR and numbers of cardiometabolic risks in non-diabetic patients and speculated that such relationships could also be observed in diabetic patients. In the case of increased sympathetic activity and metabolism, oxidative stress and inflammation also increase,[57,58] and participate in the regulation of BRS in health or disease status.[59] BRS is a key mechanism of neuromodulation in the cardiovascular system and is considered a predictor of cardiovascular events,[60] and low cardiovagal activity and BRS are negatively correlated with increased hepatic fat content in patients with type 2 diabetes.[17] Similarly, our study confirmed that intrahepatic TG contents were associated with low cardiovagal tone and BRS in HFC-fed minipigs and exhibited obvious LV diastolic dysfunction, such as the decrease of LVEDP and LV −dp/dtmax, but had no significant effect on the contractile performance index LVSP. This was consistent with the increased risk for LV diastolic dysfunction found by Chun et al[61] in patients with NFALD. Additionally, multiple linear regression analysis also showed that low HFnu, RMSSD, BRS and LV −dp/dtmax, high NEFA, and high hepatic TG content might be the possible factors to promote the development of hepatic IR toward cardiovascular disease. Therefore, the results of this study support the evidence that hepatic IR triggers cardiovascular disorders associated with low cardiovagal tone and BRS.

5. Conclusion

This study exhibits a novel minipig model induced by feeding a HFC diet to produce intrahepatic fat deposition, hepatic IR, and cardiovascular disorders with decreased cardiovagal tone and BRS. It was proved that autonomic dysfunction is involved in the evidence that hepatic IR promotes cardiovascular diseases. Moreover, it provides a unique tool that recapitulates the link between dietary factors and hepatic IR, hypertension, and cardiovascular diseases. The results of this study also provided a new treatment strategy for hepatic IR-based cardiovascular complications, either by reducing IR and enhancing BRS through insulin sensitizer or by reducing oxidative stress to improve steatosis and inflammation through antioxidants.

Competing interests

The authors state that they have no competing interests.

Authors' contributions

MC and YP designed the research project, analyzed the data, and wrote the article. YP, YR, JH, KZ, JC, and CY performed the experiment. All authors read and approved the final manuscript.

Grants/funding

The authors gratefully acknowledge financial support from National Science Foundation of China (grant No. 31572346), Zhejiang Provincial Natural Science Foundation of China (grant No. LY16C040001), public

projects Science and Technology Department of Zhejiang Province (grant No. 2015C37106), Zhejiang Chinese Medical University Scientific Research Funds (grant No. 2015G19), Medical and Health Science and Technology Project of Zhejiang Provincial Health Commission (grant No. 2017194398).

References

1. Otto MC, Afshin A, Micha R, et al. The impact of dietary and metabolic risk factors on cardiovascular diseases and type 2 diabetes mortality in Brazil. PLoS One 2016;11, e0151503.
2. Chiavaroli L, Nishi SK, Khan TA, et al. Portfolio dietary pattern and cardiovascular disease: a systematic review and meta-analysis of controlled trials. Prog Cardiovasc Dis 2018;61:43-53.
3. Muniyappa R, Montagnani M, Koh KK, Quon MJ. Cardiovascular actions of insulin. Endocr Rev 2007;28:463.
4. Xu W, Tian M, Zhou Y. The relationship between insulin resistance, adiponectin and C-reactive protein and vascular endothelial injury in diabetic patients with coronary heart disease. Exp Ther Med 2018;16:2022-6.
5. Leung PS. The potential protective action of vitamin D in hepatic insulin resistance and pancreatic islet dysfunction in type 2 diabetes mellitus. Nutrients 2016;8:147.
6. Meshkani R, Adeli K. Hepatic insulin resistance, metabolic syndrome and cardiovascular disease. Clin Biochem 2009;42:1331-46.
7. Van Gaal LF, Mertens IL, De Block CE. Mechanisms linking obesity with cardiovascular disease. Nature 2006;444:875-80.
8. Huston JM, Ochani M, Rosas-Ballina M, et al. Splenectomy inactivates the cholinergic antiinflammatory pathway during lethal endotoxemia and polymicrobial sepsis. J Exp Med 2006;203:1623-8.
9. Borovikova LV, Ivanova S, Zhang M, et al. Vagus nerve stimulation attenuates the systemic inflammatory response to endotoxin. Nature 2000;405:458-62.
10. Brito JO, Ponciano K, Figueroa D, et al. Parasympathetic dysfunction is associated with insulin resistance in fructose-fed female rats. Braz J Med Biol Res 2008;41:804-8.
11. Pal GK, Pal P, Nanda N, Amudharaj D, Adithan C. Cardiovascular dysfunctions and sympathovagal imbalance in hypertension and prehypertension: physiological perspectives. Future Cardiol 2013;9:53-69.
12. Ewing DJ, Martyn CN, Young RJ, Clarke BF. The value of cardiovascular autonomic function tests: 10 years experience in diabetes. Diabetes Care 1985;8:491-8.
13. Imholz BP, Wieling W, van Montfrans GA, Wesseling KH. Fifteen years experience with finger arterial pressure monitoring: assessment of the technology. Cardiovasc Res 1998;38:605-16.
14. Wang W, Redline S, Khoo MC. Autonomic markers of impaired glucose metabolism: effects of sleep-disordered breathing. J Diabetes Sci Technol 2012;6:1159-71.
15. Honzikova N, Zavodna E. Baroreflex sensitivity in children and adolescents: physiology, hypertension, obesity, diabetes mellitus. Physiol Res 2016;65:879-89.
16. Shirbani F, Barin E, Lee Y, et al. Characterisation of cardiac autonomic function in multiple sclerosis based on spontaneous changes of heart rate and blood pressure. Mult Scler Relat Disord 2018;22:120-7.
17. Ziegler D, Strom A, Kupriyanova Y, et al. Association of lower cardiovagal tone and baroreflex sensitivity with higher liver fat content early in type 2 diabetes. J Clin Endocrinol Metab 2018;103:1130-8.
18. Critser JK, Laughlin MH, Prather RS, Riley LK. Proceedings of the conference on swine in biomedical research. ILAR J 2009;50:89-94.
19. Walters EM, Prather RS. Advancing swine models for human health and diseases. Mo Med 2013;110:212-5.
20. Kawaguchi H, Miyoshi N, Miura N, et al. Microminipig, a non-rodent experimental animal optimized for life science research: novel atherosclerosis model induced by high fat and cholesterol diet. Jpn J Pharmacol 2011;115:115-21.
21. Mcanulty PA, Dayan AD, Ganderup NC, Hastings KL. *The Minipig in Biomedical Research*. CRC Press. 2011.
22. Liu Z, Patil IY, Jiang T, et al. High-fat diet induces hepatic insulin resistance and impairment of synaptic plasticity. PLoS One 2015;10, e0128274.
23. Yongming P, Zhaowei C, Yichao M, et al. Involvement of peroxisome proliferator-activated receptors in cardiac and vascular remodeling in a novel minipig model of insulin resistance and atherosclerosis induced by consumption of a high-fat/cholesterol diet. Cardiovasc Diabetol 2015;14:6.
24. Canadas L, Ruiz JR, Veiga OL, et al. Obese and unfit students dislike physical education in adolescence: myth or truth? The AVENA and UP&DOWN studies. Nutr Hosp 2014;30:1319-23.
25. Winn NC, Vieira-Potter VJ. Loss of UCP1 exacerbates Western diet-induced glycemic dysregulation independent of changes in body weight in female mice. Am J Physiol Regul Integr Comp Physiol 2017;312:R74-84.
26. Christoffersen B, Ribel U, Raun K, Golozoubova V, Pacini G. Evaluation of different methods for assessment of insulin sensitivity in Gottingen minipigs: introduction of a new, simpler method. Am J Physiol Regul Integr Comp Physiol 2009;297:R1195-201.
27. Wainright KS, Fleming NJ, Rowles JL, et al. Retention of sedentary obese visceral white adipose tissue phenotype with intermittent physical activity despite reduced adiposity. Am J Physiol Regul Integr Comp Physiol 2015;309:R594-602.
28. Wang SH, Wang YZ, Zhang KY, Shen JH, Zhou HQ, Qiu XY. Effect of superoxide dismutase and malondialdehyde metabolic changes on carcinogenesis of gastric carcinoma. World J Gastroenterol 2005;11:4305-10.
29. Kuwahara M, Tsujino Y, Tsubone H, Kumagai E, Tsutsumi H, Tanigawa M. Effects of pair housing on diurnal rhythms of heart rate and heart rate variability in miniature swine. Exp Anim 2004;53:303-9.
30. Voss L, Bolton D, Galland B, Taylor B. Endotoxin effects on markers of autonomic nervous system function in the piglet: implications for SIDS. Biol Neonate 2004;86:39-47.
31. Deol P, Evans JR, Dhahbi J, et al. Soybean oil is more obesogenic and diabetogenic than coconut oil and fructose in mouse: potential role for the liver. PLoS One 2015;10, e0132672.
32. Jornayvaz FR, Samuel VT, Shulman GI. The role of muscle insulin resistance in the pathogenesis of atherogenic dyslipidemia and nonalcoholic fatty liver disease associated with the metabolic syndrome. Annu Rev Nutr 2010;30:273-90.
33. Ross R, Dagnone D, Jones PJH, et al. Reduction in obesity and related comorbid conditions after diet-induced weight loss or exercise-induced weight loss in men: a randomized, controlled trial. Ann Intern Med 2000;133:92-103.
34. Mather K. Surrogate measures of insulin resistance: of rats, mice, and men. Am J Physiol Endocrinol Metab 2009;296:E398.
35. Gastaldelli A, Cusi K, Pettiti M, et al. Relationship between hepatic/visceral fat and hepatic insulin resistance in nondiabetic and type 2 diabetic subjects. Gastroenterology 2007;133:496-506.
36. DeFronzo RA. Dysfunctional fat cells, lipotoxicity and type 2 diabetes. Int J Clin Pract Suppl 2004;143:9-21.
37. Haus JM, Solomon TP, Marchetti CM, Edmison JM, Gonzalez F, Kirwan JP. Free fatty acid-induced hepatic insulin resistance is attenuated following lifestyle intervention in obese individuals with impaired glucose tolerance. J Clin Endocrinol Metab 2010;95:323-7.
38. Ford ES. Body mass index, diabetes, and C-reactive protein among U.S. adults. Diabetes Care 1999;22:1971-7.
39. Akash MSH, Rehman K, Liaqat A, Numan M, Mahmood Q, Kamal S. Biochemical investigation of gender-specific association between insulin resistance and inflammatory biomarkers in types 2 diabetic patients. Biomed Pharmacother 2018;106:285-91.
40. Mlinar B, Marc J, Janez A, Pfeifer M. Molecular mechanisms of insulin resistance and associated diseases. Clin Chim Acta 2007;375:20-35.
41. Riley JK, Carayannopoulos MO, Wyman AH, Chi M, Moley KH. Phosphatidylinositol 3-kinase activity is critical for glucose metabolism and embryo survival in murine blastocysts. J Biol Chem 2006;281:6010.
42. Stahel P, Kim J, Cieslar S, Warrington J, Xiao C, Cant J. Supranutritional selenium intake from enriched milk casein impairs hepatic insulin sensitivity via attenuated IRS/PI3K/AKT signaling and decreased PGC-1α expression in male Sprague-Dawley rats. J Nutr Biochem 2017;41:142-50.
43. Xu H, Zhou Y, Liu YX, et al. Metformin improves hepatic IRS2/PI3K/Akt signaling in insulin resistant rats of NASH and cirrhosis. J Endocrinol 2016;229:133.
44. Pearce NJ, Arch JR, Clapham JC, et al. Development of glucose intolerance in male transgenic mice overexpressing human glycogen synthase kinase-3beta on a muscle-specific promoter. Metabolism 2004;53:1322-30.
45. Sakamaki J, Daitoku H, Kaneko Y, Hagiwara A, Ueno K, Fukamizu A. GSK3beta regulates gluconeogenic gene expression through HNF4alpha and FOXO1. J Recept Signal Transduct Res 2012;32:96-101.
46. Bouzakri K, Roques M, Gual P, et al. Reduced activation of phosphatidylinositol-3 kinase and increased serine 636 phosphorylation of insulin receptor substrate-1 in primary culture of skeletal muscle cells from patients with type 2 diabetes. Diabetes 2003;52:1319-25.
47. Tzatsos A, Kandror KV. Nutrients suppress phosphatidylinositol 3-kinase/Akt signaling via raptor-dependent mTOR-mediated insulin receptor substrate 1 phosphorylation. Mol Cell Biol 2006;26:63-76.
48. Crunkhorn S, Dearie F, Mantzoros C, et al. Peroxisome proliferator activator receptor γ coactivator-1 expression is reduced in obesity. J Biol Chem 2007;282:15439-50.
49. Sookoian S, Rosselli MS, Gemma C, et al. Epigenetic regulation of insulin resistance in nonalcoholic fatty liver disease: impact of liver methylation of the peroxisome proliferator-activated receptor γ coactivator 1α promoter. Hepatology 2010;52:1992-2000.
50. Burgueno AL, Cabrerizo R, Gonzales Mansilla N, Sookoian S, Pirola CJ. Maternal high-fat intake during pregnancy programs metabolic-syndrome-related phenotypes through liver mitochondrial DNA copy number and transcriptional activity of liver PPARGC1A. J Nutr Biochem 2013;24:6-13.
51. Saito I, Takata Y, Maruyama K, et al. Association between heart rate variability and home blood pressure: the Toon Health Study. Am J Hypertens 2018;31:1120-6.
52. Kiviniemi AM, Tulppo MP, Wichterle D, et al. Novel spectral indexes of heart rate variability as predictors of sudden and non-sudden cardiac death after an acute myocardial infarction. Ann Med 2007;39:54-62.
53. Thayer JF, Yamamoto SS, Brosschot JF. The relationship of autonomic imbalance, heart rate variability and cardiovascular disease risk factors. Int J Cardiol 2010;141:122-31.
54. Jakovljevic DG, Hallsworth K, Zalewski P, et al. Resistance exercise improves autonomic regulation at rest and haemodynamic response to exercise in non-alcoholic fatty liver disease. Clin Sci (Lond) 2013;125:143-9.
55. Yi CX, Sefliers LF. The role of the autonomic nervous liver innervation in the control of energy metabolism. Biochim Biophys Acta 2010;1802:416.
56. Targher G, Bertolini L, Rodella S, et al. NASH predicts plasma inflammatory biomarkers independently of visceral fat in men. Obesity (Silver Spring) 2008;16:1394-9.
57. Cikrikcioglu MA, Hursitoglu M, Erkal H, et al. Oxidative stress and autonomic nervous system functions in restless legs syndrome. Eur J Clin Invest 2011;41:734-42.
58. Topp H, Fusch G, Schoch G, Fusch C. Noninvasive markers of oxidative DNA stress, RNA degradation and protein degradation are differentially correlated with resting metabolic rate and energy intake in children and adolescents. Pediatr Res 2008;64:246-50.
59. Chapleau MW, Li Z, Meyrelles SS, Ma X, Abboud FM. Mechanisms determining sensitivity of baroreceptor afferents in health and disease. Ann N Y Acad Sci 2001;940:1-19.
60. Johansson M, Gao SA, Friberg P, et al. Baroreflex effectiveness index and baroreflex sensitivity predict all-cause mortality and sudden death in hypertensive patients with chronic renal failure. J Hypertens 2007;25:163-8.
61. Chung GE, Lee J-H, Lee H, et al. Nonalcoholic fatty liver disease and advanced fibrosis are associated with left ventricular diastolic dysfunction. Atherosclerosis 2018;272:137-44.